Journal of Oceanology and Limnology
Vol. 41 No. 3, P. 1109-1121, 2023
https://doi.org/10.1007/s00343-022-2129-7

Oyster studies reveal the duplication and functional diversification of Bivalvia caspase-8 genes*

Shaoxi DENG[1, 2, #], Tao QU[1, 4, #], Guofan ZHANG[1, 2, 3], Fei XU[1, 2, 3 **]

[1] *CAS and Shandong Province Key Laboratory of Experimental Marine Biology, Center for Ocean Mega-Science, Institute of Oceanology, Chinese Academy of Sciences, Qingdao 266071, China*

[2] *University of Chinese Academy of Sciences, Beijing 100049, China*

[3] *Laboratory for Marine Biology and Biotechnology, Qingdao National Laboratory for Marine Science and Technology, Qingdao 266000, China*

[4] *NHC Key Laboratory of Diagnosis and Therapy of Gastrointestinal Tumor, Gansu Provincial Hospital, Lanzhou 730000, China*

Received Mar. 20, 2022; accepted in principle Apr. 11, 2022; accepted for publication Apr. 15, 2022

Abstract Caspase-8, first classified as a pro-apoptotic caspase, is considered to have arisen from duplication with caspase-10 and involves multiple immune and inflammatory responses in mammals. However, few are known on the phylogeny and function of caspase-8 in molluscs, one of the largest phyla in marine invertebrates. In this study, we conducted phylogenetic and functional analysis on molluscan caspase-8-like genes. Results indicate that duplication occurred in molluscan caspase-8-like genes, resulting in at least two caspase-8 copies in some groups of bivalves. Additional studies in Pacific oyster *Crassostrea gigas* showed different spatio-temporal expression patterns and subcellular localizations of *CgCaspase-8-1* and *CgCaspase-8-2*. While no interaction was observed between CgCaspase-8-2 and CgFADD, the adaptor molecule in apoptosis, yeast two-hybrid and co-immunoprecipitation assays suggested the interaction between CgCaspase-8-1 and CgFADD, indicating its pro-apoptotic function. In addition, CgCaspase-8-1 showed interaction with the CARD domain of CgRIG-I. Together with two NF-κB subunits (Cgp105 and CgRel), their transcripts were up-regulated in response to poly(I:C) stimuli, supporting the immune function of both pro- and anti-inflammation. The results provide insight into the evolution and functional diversification of Bivalvia caspase-8 genes.

Keyword: caspase-8; apoptosis; metamorphosis; inflammation; *Crassostrea gigas*

1 INTRODUCTION

Cell death as a pervasive physiological phenomenon plays crucial roles in the development of multicellular organisms. Cell death can be classified into different modes according to the morphological characterization: apoptosis, autophagy, necrosis, mitotic catastrophe, and others (Galluzzi et al., 2007; Green and Llambi, 2015). Apoptosis is further classified as extrinsic and intrinsic (Kerr et al., 1972; Galluzzi et al., 2012). Extrinsic apoptosis is predominantly initiated by the binding of lethal ligands and death receptors (DRs, e.g., FAS/CD95, TNFα receptor 1 (TNFR1), and TRAIL receptor (TRAILR) 1-2), resulting the activation of initiator caspases (caspase-8 or -10) and a cascade activation of executioner caspases (Ashkenazi and Dixit, 1998; Wajant, 2002; Bladon and Taylor, 2006; Schütze et al., 2008).

Caspases, the interleukin-1β-converting enzyme family proteases, are the key component of apoptotic pathways. They are classified as initiator (caspase-2, -8, -9, -10) and executioner caspases (caspase-3, -6, -7) (Fan et al., 2005; Launay et al., 2005; Vogeler et al., 2021). One typical form of the death reporter

* Supported by the Science & Technology Innovation Project of Laoshan Laboratory (No. LSKJ202203001), the Center for Ocean Mega-Research of Science, Chinese Academy of Sciences (No. COMS2019Q11), the GHfund B (No. 20210702), and the Taishan Scholars Program

** Corresponding author: xufei@qdio.ac.cn

# Shaoxi DENG and Tao QU contributed equally to this work and should be regarded as co-first authors.

signaling is initiated by FAS ligation, which results the activation of extrinsic apoptosis. Trimerizated death receptors recruit the receptor-specific adapter protein FAS-associated death domain (FADD) and other proteins to construct a "death-inducing signaling complex" (DISC), which then recruits and activates procaspase-8 (or -10) to initiate the apoptosis (Boldin et al., 1995; Kruidering and Evan, 2000; Wang et al., 2001; Lavrik et al., 2005). The caspase-8 protein also plays an important role in the innate immune system. It directly binds to pattern recognition receptors (PRRs) retinoic acid-inducible gene I (RIG-I) to activate the mitochondrial antiviral signaling protein (MAVS) - dependent RIG-I-like receptor (RLR) signaling pathway, and further activates the downstream NF-κB and interferon signaling (Takeuchi and Akira, 2010; Rajput et al., 2011; Roth et al., 2011).

Pacific oyster *Crassostrea gigas* belongs to the phylum Mollusca, the most speciose phylum of marine invertebrates. It is a dominant cultivated shellfish and a model for Spiralian evolution and marine environmental studies (Hedgecock et al., 2005). To date, a *CgCaspase-8* (i.e., *CgCaspase-8-2*), *CgCaspase-2*, *CgCaspase-1*, *CgCaspase-3*, *CgFADD*, and a potential bivalve specific group of *caspase-3*/*7* genes have been identified in *C. gigas* (Zhang et al., 2011; Qu et al., 2014; Li et al., 2015, 2016; Lu et al., 2017). *ChCaspase-8* and *ChCaspase-3* genes were also identified in *C. hongkongensis*, while *CaCaspase-2* and *CaCaspase-3* were identified in *C. angulata* (Xiang et al., 2013; Yang et al., 2015; Qin et al., 2020). Recent phylogenetic analysis of Bivalvia caspases revealed the novelty and complexity in the bivalve caspase family (Vogeler et al., 2021). However, the phylogeny analysis within Mollusca and the functional evolution of each caspase gene still need further studies.

In this study, we report that caspase-8 is under different evolution trajectories among different mollusk groups, where duplication should have occurred in some Bivalve groups. Compared with the previously reported *CgCaspase-8-2* (Li et al., 2015), *CgCaspase-8-1* showed different expression and molecular interaction patterns, indicating functional diversification post duplication.

2 MATERIAL AND METHOD

2.1 Animal treatment and sampling

Oyster embryo and larvae collections were conducted as described in the previous report (Zhang et al., 2012). In brief, Pacific oysters were conditioned and cultured in the hatchery at Yantai, Shandong Province, China. Gametes were strip-collected from matured animals for artificial insemination. Eggs, embryos, and larvae were collected and preserved in liquid nitrogen. Fresh samples from different tissues of adult oysters were also collected and fixed for gene expression analysis. When 90% larvae reached the pediveliger stage (about two weeks post-fertilization), relatively uniform-sized larvae were selected with mesh screening and treated 20 min with epinephrine hydrochloride (YuanyeBio, China) at the final concentration of 1×10^{-4} mol/L (Coon et al., 1986). The induced larvae were transferred into fresh seawater, and larval samples at different time points post-treatment were collected and preserved in liquid nitrogen.

Adult oysters for the immune challenge were from an oyster farm in Qingdao, Shandong Province, China. Animals were acclimated in aerated and filtered seawater at 20±1 ℃ for one week while periodically feeding and changing the water. A total of 240 oysters were randomly selected to punch a small hole on the backward of shells around the adductor muscle. The treated oysters were randomly divided into three groups and recovered in fresh seawater for 24 h before the immune challenge. Oysters in the poly(I:C) and PBS experimental groups were injected with 100-μL poly(I:C) (Invivogen, France) suspended in phosphate buffer solution (PBS, CellWorld, China) at a final concentration of 1 mg/mL and 100-μL PBS respectively, while those in the control group were cultured without any treatment. Hemolymph samples of 12 oysters from each group were collected per sampling time and fixed in liquid nitrogen for gene expression analysis.

2.2 Phylogenetic analysis of mollusc caspase-8 genes

The specific primers casp8-1F and casp8-1R (Supplementary Table S1) were designed to obtain the open reading frame (ORF) of *CgCaspase-8-1*, according to the deduced gene model (GenBank accession number: CGI_10003767) from the *C. gigas* genome. The ExPASy compute pI/Mw tool was used to calculate the molecular mass and the theoretical isoelectric point (pI/Mw) (Bjellqvist et al., 1993, 1994; Gasteiger et al., 2005). The conserved protein domains were predicted with the SMART (Simple Modular Architecture Research Tool) and the ScanProsite (de Castro et al., 2006; Letunic et al., 2021). The novel, un-gapped motifs (recurring, fixed-length patterns) were analyzed by the MEME (Multiple EM for Motif Elicitation) and were then

visualized with IBS (Illustrator for Biological Sequences) (Ren et al., 2009; Liu et al., 2015). The Needleman-Wunsch global alignment algorithm was applied to conduct pairwise sequence alignment of the full length of *CgCaspase-8-1* and *CgCaspase-8-2*.

Caspase-8/-10 protein sequences (Supplementary Table S2) of typical species were downloaded from the NCBI database or the MolluscDB (Liu et al., 2021) for phylogenetic analysis, with caspase-2 as an outgroup. Multiple sequence alignment was performed by MAFFT (version 7) with L-INS-i algorithm (Katoh and Standley, 2013), and then trimmed with TrimAl (Capella-Gutiérrez et al., 2009), with parameters -gt 0.9 -st 0.001 -cons 40. Molecular phylogenetic trees were constructed by Markov-chain Monte Carlo analysis with MrBayes 3.2.7 (Ronquist et al., 2012) under fixed(lg) model for three million generations. Evolview kit was used to visualize the output tree (Subramanian et al., 2019).

2.3 RNA isolation, cDNA synthesis, and quantitative PCR analysis

Total RNA of developmental and tissue samples was isolated according to the procedural guidelines of TRIzol reagent (Ambion, USA), while hemolymph was extracted using RNAsimple Total RNA Kit (Tiangen, China). cDNA synthesis was implemented in a 20-μL reaction mixture using Evo M-MLV RT mix kit with gDNA clean (Accurate Biology, China), in which 1 μg of total RNA was used as a template. The real-time reverse transcript polymerase chain reaction (qRT-PCR) was performed in a QuantStudio 6 Flex Real-Time PCR System (ThermoFisher, USA). The 10-μL reaction solution contained 5-μL 2× ChamQ Universal SYBR qPCR Master Mix (Vazyme, China), 1-μL forward and reverse primers mix (5 μmol/L each), and 1-μL diluted cDNA. The ribosomal protein S18 (RS18) gene was used as the internal control (Li et al., 2015). The primer sequences were listed in Supplementary Table S1 together with other primers used in this study. The relative mRNA expression level was calculated by the $2^{-\Delta\Delta Ct}$ method. The egg and hepatopancreas expression levels were used as the reference for developmental and tissue samples, respectively.

2.4 Subcellular localization assay in HeLa cells

The ORF with part of untranslated regions (UTRs) of *CgCaspase-8-1* was amplified using Taq DNA polymerase (GDSBio, China) with primers casp8-1-F2 and casp8-1-R2. The purified PCR products were fused into linearized vectors pMD19-T (TaKaRa, Japan), and the recombinant plasmids were transfected into Trelief 5α chemically competent cells (Tsingke, China). The depurated CgCasp8-1-pMD19T plasmids were sequencing verified and used as the template to perform PCR with primers Casp8-1-GFP-F and Casp8-1-GFP-R to produce expression plasmids with the mammalian expression vector pEGFP-N1 (Clontech, USA). Purified PCR products were then cloned into the EcoR I (TaKaRa, Japan) linearized vector using the ClonExpress II one step cloning kit (Vazyme, China) according to the manufacturer's protocol. The recombinant CgCasp8-1-pEGFP-N1 plasmids were recovered using endo-free plasmid DNA mini kit (Omega, USA), and transfected into ~60% confluence HeLa cells (ATCC, Manassas, USA) with ExFect transfection reagent (Vazyme, China) following the manufacturer's protocol. After 48-h culture, the nuclei were stained with Hoechst 33342 staining solution (Yuanyebio, China) after twice washing in PBS. The fluorescent signal was observed directly under a Laser-Scanning Confocal Microscopy System LSM 710 (Zeiss, Jena, Germany).

2.5 Yeast two-hybrid assay

The entire ORF and region covering the two death effector domains (DED) of *CgCaspase-8-1*, the full length of *CgFADD*, and the CARD domain of *CgRIG-I* were amplified with specific primers (Supplementary Table S1) using KOD DNA polymerase (TOYOBO, USA). Cys414 site was mutated to glycine (C414G, CgCaspase-8-1m) to prevent the proteolytic activity (Besnault-Mascard et al., 2005). The linearized plasmids pGBKT7 and pGADT7 (Clontech) were fused with PCR fragments using the In-Fusion HD Cloning Kit (Clontech, USA). The yeast two-hybrid (Y2H) assays were performed according to the protocol of Matchmaker Gold Yeast Two-Hybrid System (TaKaRa Bio, USA). The GAL4 DNA-BD Vector pGBKT7 was transfected into Y2HGold yeast strain, while the GAL4 AD Vector pGADT7 was transfected into Y187 yeast strain. The Y2HGold yeast cells and Y187 yeast cells were then spread evenly over the synthetically defined (SD) plates lacking leucine (SD/-Leu) or lacking tryptophan (SD/-Trp), respectively, and cultured at 30 °C for 3–5 d. The single colonies on -Trp and -Leu plates were selected into 2× yeast extract peptone dextrose (YPDA) liquid medium and hybridized at 30 °C and 250 r/min sharking for 20–24 h. For the visualization of interactions between proteins, the post-hybridization yeast strains were spread on double dropout (SD/-Leu/

-Trp) plates and quadruple drop-out (SD/-Ade/-His/-Leu/-Trp) plates supplemented with X-α-Gal and Aureobasidin A (TaKaRa), respectively.

2.6 Co-immunoprecipitation (Co-IP) assays

The plasmid pCMV-Myc (Clontech, USA) was linearized by EcoRI (New England Biolabs, USA) to construct -myc fusion protein, while the plasmid pCMS-EGFP-FLAG (Huang et al., 2019) digested with XhoI (New England Biolabs) was used to construct the -flag fusion protein. Purified PCR products were cloned into the linearized vectors using the In-Fusion HD Cloning Kit (Clontech, USA). HEK293T cells (ATCC, Manassas, USA) were placed into cell culture plates (100-mm diameter). Two recombinant expression plasmids, pCMV-Myc (Clontech, USA) and pCMS-EGFP-FLAG, were co-transfected in a ratio of 1∶1 when cells were 60%–80% confluence. After culturing for 24 h, the cells were harvested and washed in PBS. Cell lysis buffer (Beyotime, China) was added to lyse the cells for 30 min. After centrifuging the cell lysate, 30 μL of the supernatant was taken to prepare the input samples, while the remaining supernatant was incubated with balanced anti-FLAG M2 magnetic beads (Sigma, USA) under gentle shaking at 4 °C for 2–4 h to prepare the Co-IP samples. Before western blotting (WB) detection, the input and Co-IP samples were incubated at 100 °C for 3–5 min with 2× loading buffer for protein sodium dodecyl sulfate polyacrylamide gel electrophoresis (TaKaRa). The samples were assayed using anti-Myc (Roche, Switzerland) and anti-FLAG antibodies (Sigma), while the input sample was treated with anti-Myc antibody as a negative control.

2.7 Dual-Luciferase reporter assay

The Dual-Luciferase reporter assays were performed to analyze the influence of CgCaspase-8-1 on the activation of NF-κB signaling pathway. The mammalian expression plasmid CgCasp8-1-pSI containing only the ORF region was constructed with a similar process described in the subcellular location assay. HEK293T cells were transferred and cultured in 96-well plates. The expression vector and firefly luciferase reporter vectors with NF-κB promoter (pGL6-NF-κB-luc, Beyotime Biotechnology Corporation, China) and pRL-CMV *Renilla* luciferase vector (control vector, Promega, USA) were co-transfection into 60%–80% confluent HEK293T cells. The luminescence of firefly and *Renilla* was measured using Dual-Lite Luciferase Assay System (Vazyme, China) at 24-h post-transfection.

2.8 Statistical analysis

All assays were performed with triplicate or quadruplicate technical and biological replicates as shown in the results part. The data were analyzed with one-way analysis of variance (ANOVA) and Fisher's least significant difference (LSD) using IBM SPSS Statistics 25. The thresholds for significant and highly significant levels were set at $P<0.05$ and $P<0.01$.

3 RESULT

3.1 Sequence characteristics of CgCaspase-8-1

The ORF of *CgCaspase-8-1* is 1 668 bp encoding a deduced protein of 555 amino acids, with a potential molecular mass of 63.15 kDa and a predicted isoelectric point at 6.11. The conserved domains analysis showed that CgCaspase-8-1 contained two DED domains (amino acid site: D8-G86 and E105-Q185), a caspase family P20 large subunit and a P10 small subunit (P295-S419 and A460-K554). At the same time, a caspase family histidine active site 'HSQFDCLVFCILSHG' (H359-G373) and a cysteine active site 'KPKLFFFQACQG' (K406-G417) are represented in the CgCaspase-8-1 sequence as well (Fig.1). Pairwise sequence alignment of CgCaspase-8-1 and CgCaspase-8-2 showed that nucleotide and amino acid sequences shared low percentages of identities and similarities (nucleotide sequence: 37.8% and 37.8%, amino acid sequence: 27.9% and 42.1%, respectively, Table 1). Novel motifs analysis by MEME also indicated tremendous motif distribution difference between CgCaspase-8-1 and CgCaspase-8-2 (Fig.1). However, CgCaspase-8-1 showed high similarity with the reported *C. hongkongensis* ChCaspase-8 (Xiang et al., 2013).

Further comparison revealed the low identities of CgCaspase-8-1 with caspase-8s from selected species: *Xenopus tropicalis* (28%), *Danio rerio* (30%), *Homo sapiens* (32%), *Gallus gallus* (32%), *Branchiostoma floridae* (31%), *Mytilus galloprovincialis* (42%), and caspase-10s of selected craniates: *Gallus gallus* (33%), *Xenopus tropicalis* (31%), *Homo sapiens* (36%). However, the caspase-8/10 active site "QACQG" showed a high identity among all selected species (Supplementary Fig.S1).

3.2 Phylogenetic analysis of Caspase-8 proteins

Phylogenetic analysis showed that caspase-8/-10 members from each of the three Bilaterian clades were grouped with high posterior probability supports, where the vertebrates' caspase-8 and -10 were closely

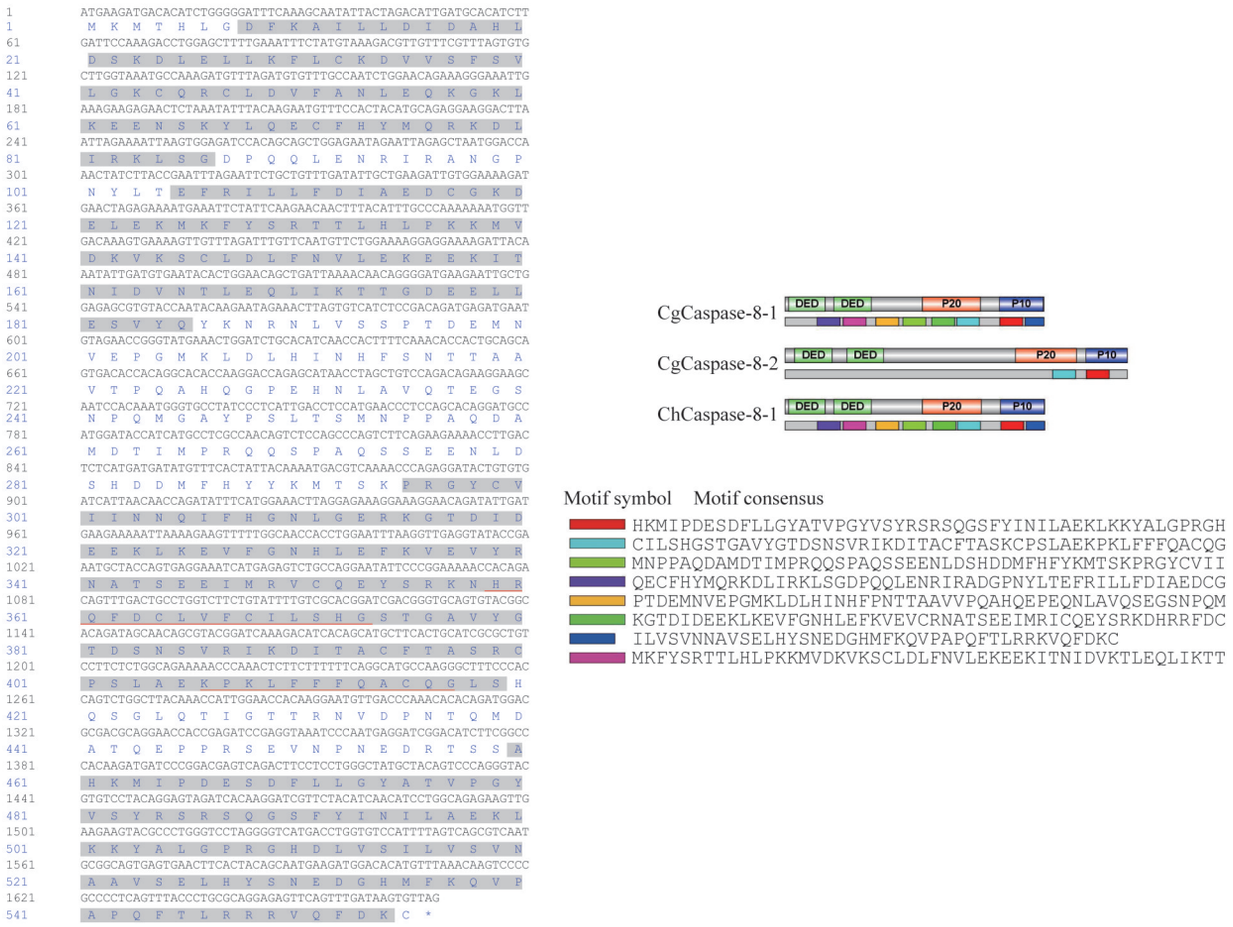

Fig.1 Characterizations of nucleotide and deduced amino acid sequences of oyster caspase-8

a. nucleotide and deduced amino acid sequences of CgCaspase-8-1. The two DED domains, P20 large subunit and P10 small subunit were shaded. The histidine active site 'HSQFDCLVFCILSHG' and cysteine active site 'KPKLFFFQACQG' were highlighted with underlines. b. diagram showing the conserved protein domains and novel motifs of CgCaspase-8-1, CgCaspase-8-2, and ChCaspase-8. Different domains and motifs were distinguished with different labels and colors.

Table 1 Pairwise sequence alignment of CgCaspase-8-1 and CgCaspase-8-2

	Identity (%)	Similarity (%)	Gap (%)
Amino acid	27.9	42.1	32.6
Nucleotide	37.8	37.8	51.9

clustered. Homologs from most assayed bivalves were divided into two clades suggesting gene duplication, while only one copy was identified in all the investigated Gastropoda genomes (Fig.2).

3.3 Expression pattern of *CgCaspase-8-1* in larval and adult oysters

Real-time quantitative PCR analysis showed the high expression level of *CgCaspase-8-1* during the early development stages. The gene expression levels increased shortly after fertilization, almost seven-fold higher at the four-cell stage than the egg. The high expression level lasted till the early morula stage, followed by a descent to D-shape larvae (Fig.3a). Previously reported RNAseq data (Zhang et al., 2012) indicated a slight increase in later development stages (Fig.3b). Female gonad had the most expression level compared with other tissues, possibly because of high egg content in the gonad tissue (Fig.3c). To investigate the expression profile of *CgCaspase-8-1* during metamorphosis, we induced the metamorphosis of competent pediveliger with epinephrine solution. The result indicated a slight *CgCaspase-8-1* decrease after treatment, while *CgCaspase-8-2* did not show an obvious response pattern (Fig.3d).

3.4 CgCaspase-8-1 interaction with CgFADD and CgRIG-I

In vertebrates' extrinsic apoptotic pathway, the activated death receptors recruit the FADD and

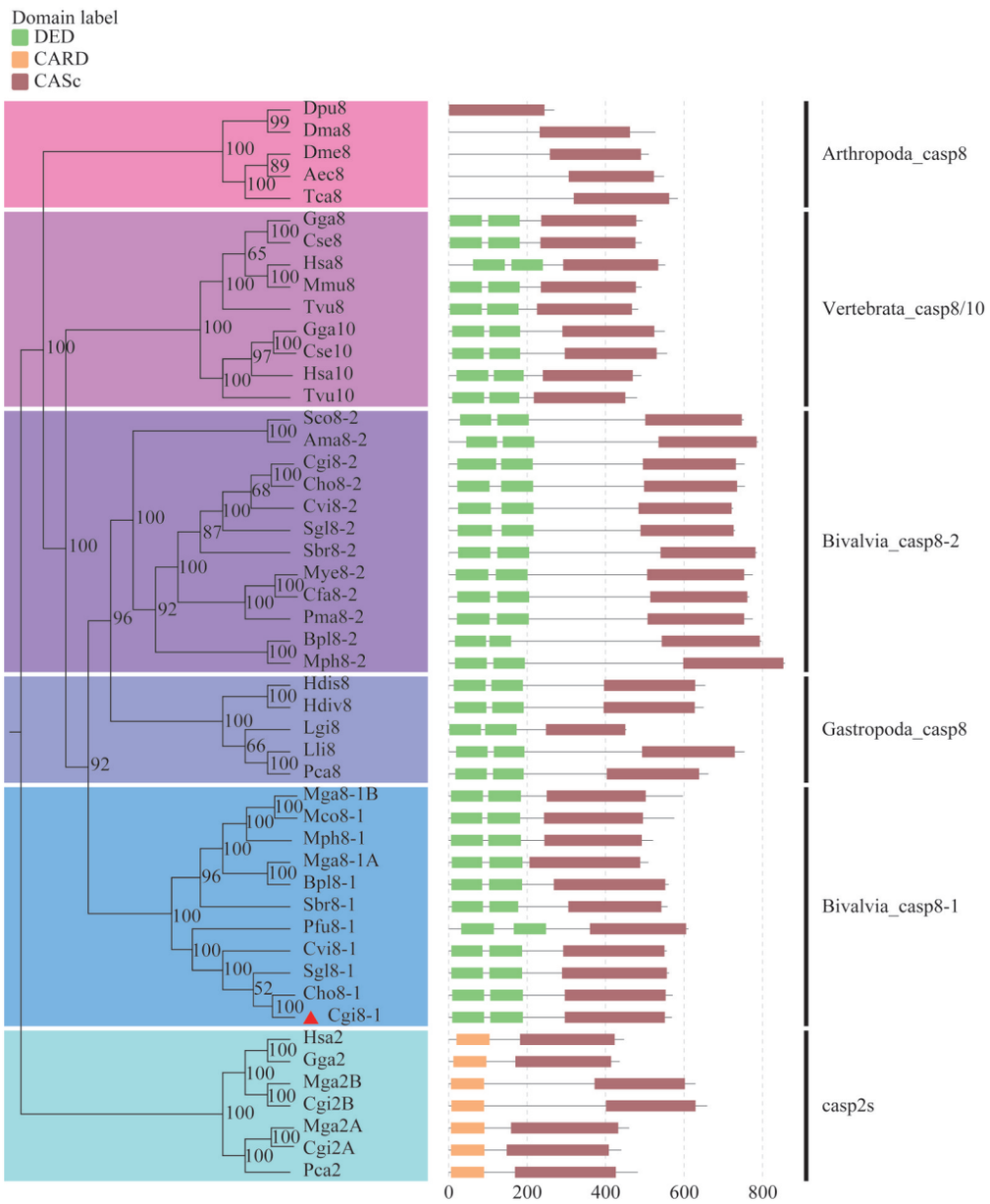

Fig.2 The bayesian phylogenetic tree of caspase-8s

The node labels represent percentage of probability. CgCaspase-8-1 is marked with the red triangle. The domains are shown in different colors. Dotted lines represent the ruler of sequence length. Species details are listed in Supplementary Table S2.

procaspase-8 to form a DISC by dimerization of the death effector domain. We thus used Y2H and Co-IP assays to validate the interaction between CgCaspase-8-1 and CgFADD. The subcellular location of CgCaspase-8-1 was firstly examined, and the results revealed both cytoplasm and nucleus location (Fig.4a). Y2H assays showed that both full-length CgCaspase-8-1m and DED region could interact with CgFADD (Fig.4b). In addition, Co-IP assays performed in the HEK293T cells suggested that CgCaspase-8-1m and DED could bind to CgFADD, further supporting the interaction of CgCaspase-8-1 and CgFADD (Fig.4c).

To validate the interaction between CgCaspase-8-1 and CgRIG-I (GenBank accession number: KY630188), the caspase recruitment domain (CARD) of CgRIG-I was fused into pGBKT7 plasmid for the Y2H assays. Results also indicated a potential interaction between Cgcaspase-8-1m and CgRIG-I-CARD (Fig.4d).

3.5 CgCaspase-8-1 involves in immune response through NF-κB pathway

The immune response of *CgCaspase-8-1* was studied by mimicking viral stimulus with poly(I:C). qRT-PCR results showed that the expression level of

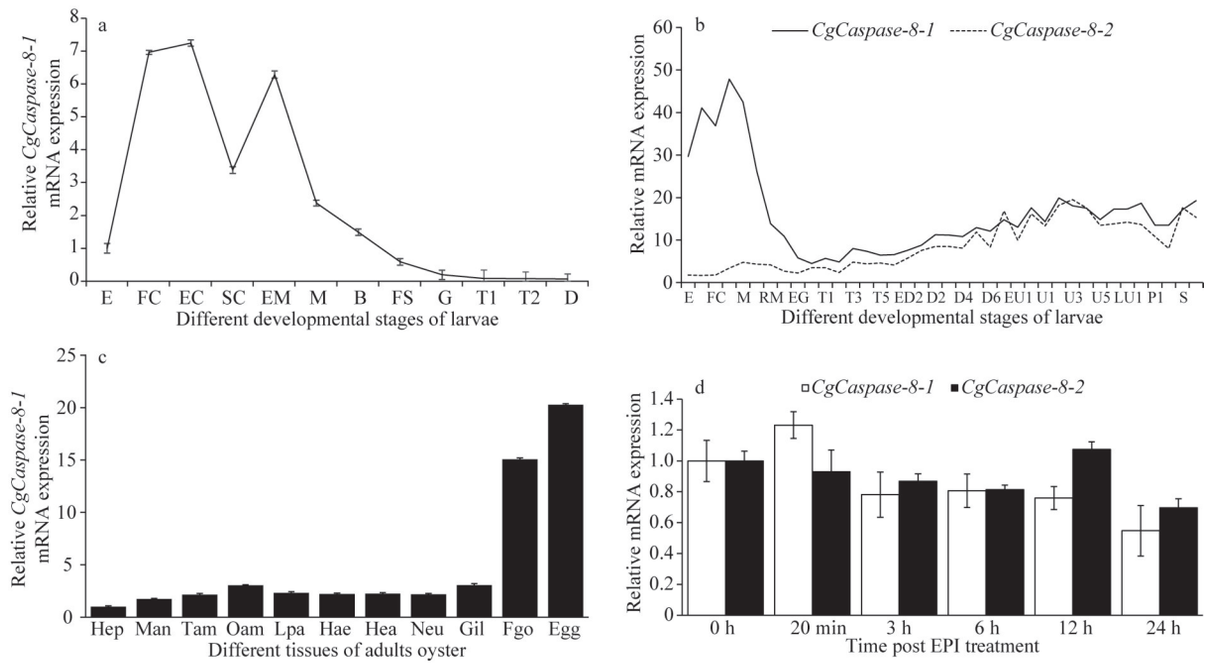

Fig.3 The expression analysis of Pacific oyster caspase-8 genes

a. qRT-PCR analysis (n=3 biological replicates) of *CgCaspase-8-1* in typical developmental stages within 24-h post fertilization; b. comparison of developmental RNAseq data (n=1) between *CgCaspase-8-1* and *CgCaspase-8-2*. The raw data were from previous report (Zhang et al., 2012); c. qRT-PCR analysis (n=3 biological replicates) of *CgCaspase-8-1* in typical adult tissues; d. qRT-PCR analysis (n=3 biological replicates) on the expression pattern of *CgCaspase-8-1* and *CgCaspase-8-2* in epinephrine treated metamorphically competent pediveligers. E: unfertilized eggs; FC: four cells stage; EC: eight cells stage; SC: sixteen cells stage; EM: early morula; M: morula; B: blastula; RM: rotary movement; FS: free swimming stage; EG: early gastrula; G: gastrula; T: trochophore; ED: early D-shape veliger; D: D-shape veliger; EU: early umbo veliger; U: umbo veliger; LU: late umbo veliger; S: spat; Hep: hepatopancreas; Man: mantle; Tam: transparent parts of adductor muscle; Oam: opaque parts of adductor muscle; Lpa: labial palps; Hae: haemolymph; Hea: heart; Neu: neuron; Gil: gills; Fgo: female gonad; P: pediveliger. Error bars represent the mean±SD, n=3.

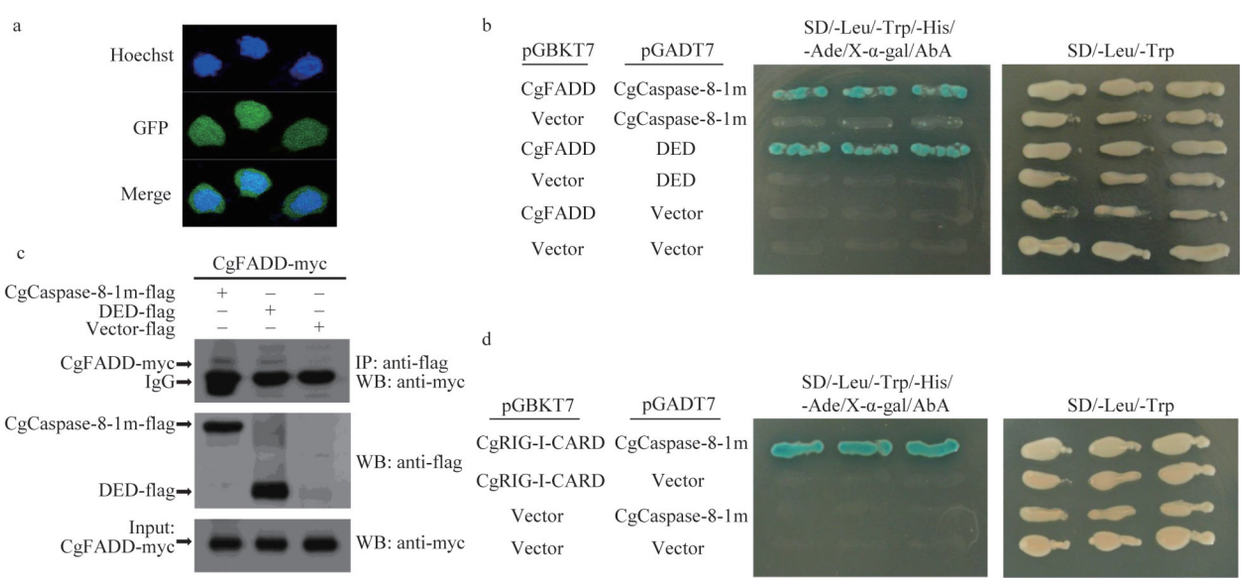

Fig.4 The subcellular localization and protein interaction analysis on CgCaspase-8-1

a. subcellular localization analysis of CgCaspase-8-1 in HeLa cells. Cell nuclei were stained by Hoechst 33342 staining solution with blue-fluorescence. CgCaspase-8-1 proteins were tagged by GFP labels with green-fluorescence; b & c. Y2H and Co-IP assays on the interaction between CgCaspase-8-1 and CgFADD. To prevent the proteolytic activity of CgCaspase-8-1 which inhibited the growth of strains, Cys414 was mutated to Gly in the sequence (C414G, CgCaspase-8-1m). Co-IP of CgCaspase-8-1m protein or DED domain with CgFADD was performed using anti-FLAG M2 magnetic beads and visualized using WB. Input samples were detected using the anti-Myc antibody as a control. CgFADD-myc was detected in Co-IP samples; d. Y2H assay on the interaction between CgCaspase-8-1 and the caspase recruitment domain (CARD) of CgRIG-I.

CgCaspase-8-1 was significantly up-regulated 24 h post-injection, and the high expression level continued till 96-h post-injection (four-fold above control, $P<0.01$, $n=4$, Fig.5a). In addition, the expression levels of *Cgp105* and *CgRel* were co-upregulated with *CgCaspase-8-1* in the hemolymph of adult oysters following poly(I:C) injection, further supporting the possible involvement of *CgCaspase-8-1* in NF-κB pathway ($n=4$, Fig.5b & c). The role of *CgCaspase-8-1* in NF- κB signaling was then investigated by the dual-luciferase reporter assays in HEK293T cells with the NF-κB reporter vector. The results indicated that the group transfected with pSI-CgCasp8-1 plasmids showed a moderate but significantly higher relative luciferase activity than the blank group (1.5× above control, $P<0.01$, $n=3$, Fig.5d).

4 DISCUSSION

In this study, we identified a caspase-8-like gene from *C. gigas* (i.e., *CgCaspase-8-1*). The gene encodes a complete caspase-8 domain, two tandem N-terminal DED domains, a C-terminal CASc domain, and a conserved cysteine active-site motif QACQG. Both sequence similarity and domain distribution of *CgCaspase-8-1* showed significant differences with the reported *C. gigas* caspase-8 gene (i.e., *CgCaspase-8-2*) (Li et al., 2015). A recent phylogenetic analysis has divided *CgCaspase-8-1* and *CgCaspase-8-2* (i.e., *Cas8A* and *Cas8B*, respectively) into different groups (Vogeler et al., 2021), indicating the existence of varying caspase-8 like homologs in Bivalvia. Intriguingly, phylogenetic analysis in this study suggests two separate caspase-8-like clades for Bivalvia but a single clade for Gastropoda. We inferred that caspase-8-like gene should have undertaken duplication independently in the common ancestor of corresponding Bivalvia species. Among the selected bivalves, *Sinonovacula constricta* and *Archivesica marissinica*, both from clade Heteroconchia, contained only *Caspase-8-2* in the genome data. Species with double copies were from clade Pteriomorphia, involving at least four orders (Ostreida, Pterioida, Arcoida, and Mytiloida). One of the caspase-8 paralogues should be absent in Pectinida as all the three assayed

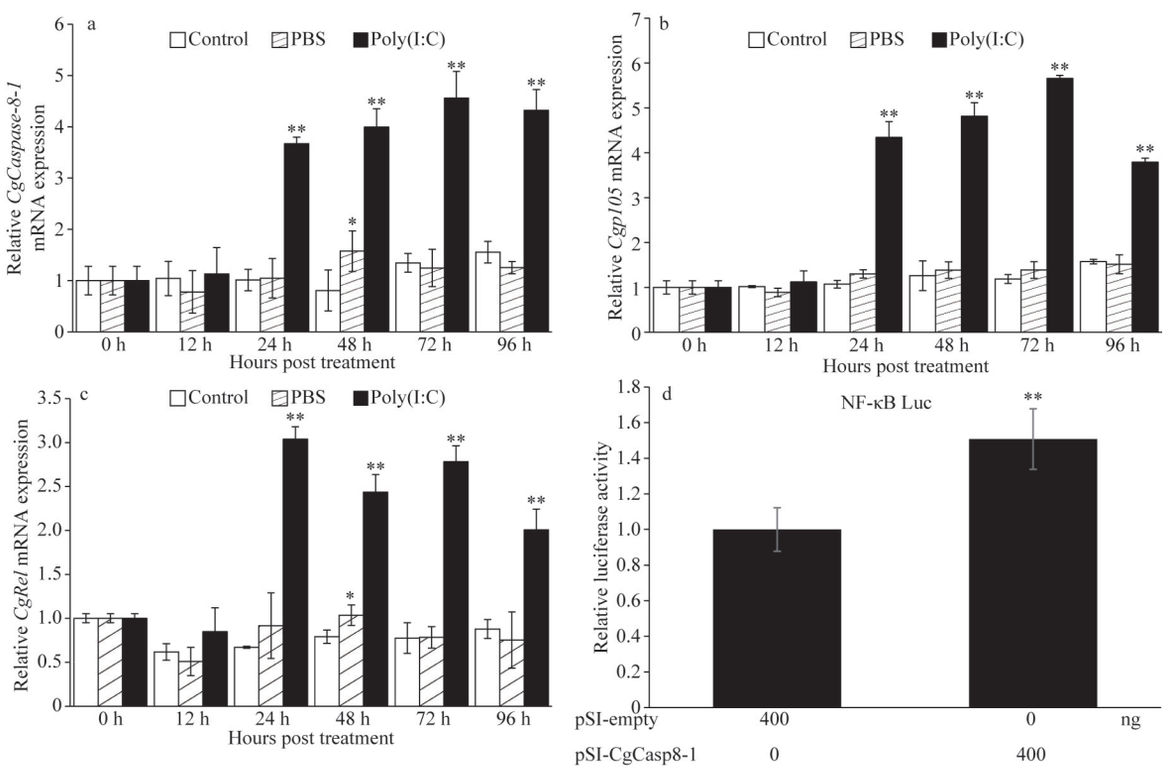

Fig.5 qRT-PCR and dual-luciferase reporter assays on the immune function of *CgCaspase-8-1*

a, b, & c. expression profile of *CgCaspase-8-1*, *Cgp105*, and *CgRel* in oyster adults following poly(I:C) challenge. Values are displayed as mean±SD ($n=4$ biological replicates). cDNA from three hemolymph samples were mixed as one template (as one biological replicate). Data were analyzed using one-way analysis of variance (ANOVA) and Fisher's least significant difference (LSD); d. dual-luciferase reporter assay of *CgCaspase-8-1* activity in the NF-κB pathway with HEK293T cells. Data were analyzed using one-way analysis of variance (ANOVA). Values are displayed as mean±SD ($n=3$). Statistically significant differences from control are labeled with ** ($P<0.01$) and * ($P<0.05$).

scallops (*Mizuhopecten yessoensis*, *Chlamys farreri*, *Pecten maximus*) contain only *Caspase-8-2*, while pearl oyster *Pinctada fucata* has only *Caspase-8-1*. We identified a possible *Caspase-8-2* (aug2.0-2134.1-15422.t1) in *P. fucata* genome, but with highly divergent sequence and motif distribution. A previous report has indicated more caspase-8-like genes in Bivalvia. But the other candidates had poor domain structures except for the two Caspase-8 genes investigated in this study (Vogeler et al., 2021). More investigations are needed to clarify the evolution of caspase-8 paralogues in Pectinida. The expansion and absence of *caspase-8* paralogues in Bivalvia remind the finding in mammals, where the mouse absent *caspase-10*, the closest paralogue of *caspase-8*. In contrast to the function compensation of *caspase-8* and *caspase-10* in humans (Puente et al., 2003), the low sequence similarity between bivalve *Caspase-8-1* and *Caspase-8-2* indicates deeper functional differentiation in terms of phylogenetic analysis.

Both RNAseq and qRT-PCR data indicate divergent expression patterns of the two CgCaspase-8 genes. *CgCaspase-8-1* showed the highest expression level in early development stages (from early cleavage to blastula), followed by a rapid decline to the lowest level at gastrula and a subsequent slow increase in later development. Correspondingly, female gonad (possibly because of the high content of eggs, Fig.3c) also showed the highest expression level among the assayed tissues. The high expression of *CgCaspase-8-1* in eggs and early development stages suggests the maternal inheritance and possible function in embryogenesis. In contrast, *CgCaspase-8-2* was in low expression level at the early development stages with a slow increase to juvenile (Fig.3b), while with the highest expression level in adult hemolymph (Li et al., 2015).

As oyster experiences veliger losses and other critical physiological changes at the metamorphosis stage, we investigated the possible involvement of the two CgCaspase-8 genes in the metamorphosis by determining their expression patterns. The results indicated different expression profiles, where *CgCaspase-8-1* showed an apparent decrease trend within 24-h post-treatment. However, the inducing efficiency of epinephrine treatment varied with the development status of pediveliger. The tested samples were complicated mixtures containing non-metamorphosis larvae. The expression dynamics indicated possible response of pediveliger to epinephrine, but was insufficient to infer the genic response during metamorphosis.

As an initiator caspase, caspase-8 triggers the extrinsic apoptosis by activating downstream executioner caspases and induces mitochondrial damage through cleaving BID, a death agonist member of the Bcl2/Bcl-xL family, in the cytoplasm (Wang et al., 1996; Salvesen and Dixit, 1997; Li et al., 1998). However, caspase-8 is not a strictly cytoplasmic protein. Studies had revealed that caspase-8 was transferred into the nucleus and inactivated PARP-2, a nuclear DNA-dependent poly (ADP-ribose) polymerase catalyzing the formation of ADP-ribose polymers in the presence of damaged DNA, in a murine model of acute ischemia (Amé et al., 1999; Benchoua et al., 2002). In addition, a report indicated that the nuclear localization of caspase-8 was associated with its sumoylation at lysine 156 (Besnault-Mascard et al., 2005). Subcellular localization study with HeLa cells showed that CgCaspase-8-1 could be detected in the cytoplasm and nucleus, different from the report in its *C. hongkongensis* ortholog (Xiang et al., 2013). This is also different from its paralog CgCaspase-8-2, which was reported to be located only in the cytoplasm (Li et al., 2015).

Extrinsic apoptosis is triggered by the binding of DRs and corresponding ligands, resulting the formation of DR signaling complex: the CD95 (Fas) and TRAILR1/TRAILR2 DISCs, as well as complex I with TNFR1 signaling (Lavrik et al., 2005). For the DISCs, the adaptor FADD recruits and activates procaspase-8 via the binding of homotypic death effector domains (DEDs). For TNFR1 signaling, two distinct signaling complexes are required to activate the apoptosis pathway: complex I forming at membrane and complex II in the cytosol. It was reported that FADD and procaspase-8 were absent in complex I, whereas complex I could transfer from membrane to cytosol and interact with FADD and procaspase-8 to construct the complex II, which leads to the activation of caspase-8 (Micheau and Tschopp, 2003). However, CgCaspase-8-2 was reported not interacting with FADD, a precondition involved in apoptosis (Li et al., 2015). We thus performed Y2H and Co-IP assays to identify the interaction between CgCaspase-8-1 and CgFADD. The results showed that yeast co-expressing CgFADD with CgCaspase-8-1m or DED could survive and develop on the quadruple drop-out (SD/-Ade/-His/-Leu/-Trp) plates, suggesting the interaction between CgCaspase-8-1 and CgFADD. Co-IP assays further validated the interaction and indicated that CgCaspase-

8-1 should function in the programmed cell death of *C. gigas* through the interaction of the N-terminal tandem DEDs with CgFADD, similar to the vertebrate. The data added adamant evidence for the existence of extrinsic apoptosis signaling (Lacoste et al., 2002; Romero et al., 2015).

The role of CgCaspase-8-1 in immune system was also investigated in this study. The overexpression of caspase-8 protein could induce the activation of NF-κB pathway in vertebrates. This property is independent of its CASc domain but instead on its two tandem N-terminal DED domains (Chaudhary et al., 2000). As CgCaspae-8-1 contains the complete caspase-8 domains, we performed qRT-PCR analysis to verify its possible involvement in NF-κB pathway. Poly(I:C) was used to mimic viral infections and assay gene response during immune stimulation (Fortier et al., 2004). The results showed co-upregulated of *CgCaspase-8-1* with two NF-κB subunits, *Cgp105* and *CgRel*, supporting the speculation on the involvement of *CgCaspase-8-1* in the immune system. The previous reports also indicated expression responses of *ChCaspase-8-1* in Hong Kong oysters under bacteria treatment (Xiang et al., 2013) and *CgCaspase-8-2* in Pacific oysters under poly(I:C) challenge (Li et al., 2015). We inferred that *CgCaspase-8-1* and *CgCaspase-8-2* should share a similar or compensation role in the aspect of immune and proinflammatory functions (Li et al., 2015). It was reported that caspase-8 acts as a scaffold for the activation of NF-κB upon TRAIL stimulation and participates in the FasL-induced NF-κB activation, which typically results in apoptosis via caspase cascade (Matsuda et al., 2014; Henry and Martin, 2017). Other studies also indicated that the heterodimers of caspase-8 and its catalytically inactive homologue, cFLIP, regulates the inflammatory cytokine gene expression upon TLR stimulation (Philip et al., 2016). Further studies are needed to confirm which pathways the two CgCaspase-8s are involved.

Once it senses microbial pathogens, the immune system constructs a large mitochondrial-associated complex in the vertebrate. The pattern recognition receptor RIG-I interacts with the mitochondrial antiviral signaling adaptor (MAVS) via two C-terminal caspase recruitment domains (CARDs) in this process (Yoneyama and Fujita, 2009). The complex contains the serine-threonine kinase receptor interacting protein 1 (RIP1) with TRADD, FADD, and caspase-8. Polyubiquitinated RIP1 subsequently assembles a signalosome containing the regulatory IKK subunit NEMO and IKK-related kinases, further regulating downstream interferon and NF-κB signaling (Roth and Ruland, 2011). Furthermore, caspase-8 can also interact directly with RIG-I (Rajput et al., 2011). The caspase-8 precursor can activate NF-κB signaling with FADD and Casper (caspase-8-related protein) when recruited to the TNFR1 complex (Hu et al., 2000). In this study, we verified the interaction between CgCaspase-8-1 and CgRIG-I. Y2H results showed that the CARD of CgRIG-I could interact with CgCaspase-8-1m. Dual-luciferase reporter assays demonstrated that when *CgCaspase-8-1* expression plasmids were transfected into mammalian cells, the reporter genes regulated with NF-κB binding motif showed moderate expression induction. These results indicated that *CgCaspase-8-1* might participate in the mollusc RLR signaling pathway and trigger the NF-κB signaling.

5 CONCLUSION

In conclusion, we identified and characterized the caspase-8-1 gene, encoding the complete caspase-8 domain in Pacific oyster *C. gigas*. Phylogenetic analysis indicated gene duplication of caspase-8-like in some groups of Bivalvia, which results in two subgroups (caspase-8-1 and caspase-8-2). Evidence suggested a significant sequence and functional differentiation between *CgCaspase-8-1* and *CgCaspase-8-2*. They have divergent expression patterns in different development stages and adult tissues. CgCaspase-8-1 localizes in the cytoplasm and nucleus, while CgCaspase-8-2 only in the cytoplasm. CgCaspase-8-1 interacts with CgFADD and should be involved in extrinsic apoptosis signaling in oysters, but CgCaspase-8-2 shows no interaction with CgFADD (Li et al., 2015). Furthermore, CgCaspase-8-1 interacts with CgRIG-I and *CgCaspase-8-1* transcripts, with two NF-κB subunits (*Cgp105* and *CgRel*) up-regulated in response to poly (I:C) stimuli, supporting the immune function of both pro- and anti- inflammation. The results reveal the evolution and function mechanism of *CgCaspase-8-1* and provide insight into the diversification of Bivalvia caspase-8 genes.

6 DATA AVAILABILITY STATEMENT

The data used and analyzed during this study are included in this article or available from the corresponding author on reasonable request.

7 ACKNOWLEDGMENT

We thank Jie MENG for her valuable suggestions and comments on this manuscript, and Oceanographic Data Center, IOCAS, for data support.

References

Amé J C, Rolli V, Schreiber V et al. 1999. PARP-2, A novel mammalian DNA damage-dependent poly(ADP-ribose) polymerase. *Journal of Biological Chemistry*, **274**(25): 17860-17868, https://doi.org/10.1074/jbc.274.25.17860.

Ashkenazi A, Dixit V M. 1998. Death receptors: signaling and modulation. *Science*, **281**(5381): 1305-1308, https://doi.org/10.1126/science.281.5381.1305.

Benchoua A, Couriaud C, Gueágan C et al. 2002. Active caspase-8 translocates into the nucleus of apoptotic cells to inactivate poly(ADP-ribose) polymerase-2. *Journal of Biological Chemistry*, **277**(37): 34217-34222, https://doi.org/10.1074/jbc.M203941200.

Besnault-Mascard L, Leprince C, Auffredou M T et al. 2005. Caspase-8 sumoylation is associated with nuclear localization. *Oncogene*, **24**(20): 3268-3273, https://doi.org/10.1038/sj.onc.1208448.

Bjellqvist B, Basse B, Olsen E et al. 1994. Reference points for comparisons of two-dimensional maps of proteins from different human cell types defined in a pH scale where isoelectric points correlate with polypeptide compositions. *Electrophoresis*, **15**(1): 529-539, https://doi.org/10.1002/elps.1150150171.

Bjellqvist B, Hughes G J, Pasquali C et al. 1993. The focusing positions of polypeptides in immobilized pH gradients can be predicted from their amino acid sequences. *Electrophoresis*, **14**(1): 1023-1031, https://doi.org/10.1002/elps.11501401163.

Bladon J, Taylor P C. 2006. Extracorporeal photopheresis: a focus on apoptosis and cytokines. *Journal of Dermatological Science*, **43**(2): 85-94, https://doi.org/10.1016/j.jdermsci.2006.05.004.

Boldin M P, Mett I L, Varfolomeev E E et al. 1995. Self-association of the "death domains" of the p55 tumor necrosis factor (TNF) receptor and Fas/APO1 prompts signaling for TNF and Fas/APO1 effects. *Journal of Biological Chemistry*, **270**(1): 387-391, https://doi.org/10.1074/jbc.270.1.387.

Capella-Gutiérrez S, Silla-Martinez J M, Gabaldon T. 2009. trimAl: a tool for automated alignment trimming in large-scale phylogenetic analyses. *Bioinformatics*, **25**(15): 1972-1973, https://doi.org/10.1093/bioinformatics/btp348.

Chaudhary P M, Eby M T, Jasmin A et al. 2000. Activation of the NF-κB pathway by caspase 8 and its homologs. *Oncogene*, **19**(39): 4451-4460, https://doi.org/10.1038/sj.onc.1203812.

Coon S L, Bonar D B, Weiner R M. 1986. Chemical production of cultchless oyster spat using epinephrine and norepinephrine. *Aquaculture*, **58**(3-4): 255-262, https://doi.org/10.1016/0044-8486(86)90090-6.

de Castro E, Sigrist C J A, Gattiker A et al. 2006. ScanProsite: detection of PROSITE signature matches and ProRule-associated functional and structural residues in proteins. *Nucleic Acids Research*, **34**(S2): W362-W365, https://doi.org/10.1093/nar/gkl124.

Fan T J, Han L H, Cong R S et al. 2005. Caspase family proteases and apoptosis. *Acta Biochimica et Biophysica Sinica*, **37**(11): 719-727, https://doi.org/10.1111/j.1745-7270.2005.00108.x.

Fortier M E, Kent S, Ashdown H et al. 2004. The viral mimic, polyinosinic: polycytidylic acid, induces fever in rats via an interleukin-1-dependent mechanism. *American Journal of Physiology-Regulatory, Integrative and Comparative Physiology*, **287**(4): R759-R766, https://doi.org/10.1152/ajpregu.00293.2004.

Galluzzi L, Maiuri M C, Vitale I et al. 2007. Cell death modalities: classification and pathophysiological implications. *Cell Death & Differentiation*, **14**(7): 1237-1243, https://doi.org/10.1038/sj.cdd.4402148.

Galluzzi L, Vitale I, Abrams J M et al. 2012. Molecular definitions of cell death subroutines: recommendations of the Nomenclature Committee on Cell Death 2012. *Cell Death & Differentiation*, **19**(1): 107-120, https://doi.org/10.1038/cdd.2011.96.

Gasteiger E, Hoogland C, Gattiker A et al. 2005. Protein identification and analysis tools on the ExPASy server. *In*: Walker J M ed. The Proteomics Protocols Handbook. Humana, Totowa. p.571-607, https://doi.org/10.1385/1-59259-890-0:571.

Green D R, Llambi F. 2015. Cell death signaling. *Cold Spring Harbor Perspectives in Biology*, **7**(12): a006080, https://doi.org/10.1101/cshperspect.a006080.

Hedgecock D, Gaffney P M, Goulletquer P et al. 2005. The case for sequencing the Pacific oyster genome. *Journal of Shellfish Research*, **24**(2): 429-441, https://doi.org/10.2983/0730-8000(2005)24[429:Tcfstp]2.0.Co;2.

Henry C M, Martin S J. 2017. Caspase-8 acts in a non-enzymatic role as a scaffold for assembly of a Pro-inflammatory "FADDosome" complex upon TRAIL stimulation. *Molecular Cell*, **65**(4): 715-729. E5, https://doi.org/10.1016/j.molcel.2017.01.022.

Hu W H, Johnson H, Shu H B. 2000. Activation of NF-κB by FADD, Casper, and caspase-8. *Journal of Biological Chemistry*, **275**(15): 10838-10844, https://doi.org/10.1074/jbc.275.15.10838.

Huang B Y, Zhang L L, Xu F et al. 2019. Oyster versatile IKKα/βs are involved in toll-like receptor and RIG-I-like receptor signaling for innate immune response. *Frontiers in Immunology*, **10**: 1826, https://doi.org/10.3389/fimmu.2019.01826.

Katoh K, Standley D M. 2013. MAFFT multiple sequence alignment software version 7: improvements in performance and usability. *Molecular Biology and Evolution*, **30**(4): 772-780, https://doi.org/10.1093/molbev/mst010.

Kerr J F R, Wyllie A H, Currie A R. 1972. Apoptosis: a basic biological phenomenon with wideranging implications in tissue kinetics. *British Journal of Cancer*, **26**(4): 239-257, https://doi.org/10.1038/bjc.1972.33.

Kruidering M, Evan G I. 2000. Caspase-8 in apoptosis: the

beginning of "the end"? *IUBMB Life*, **50**(2): 85-90, https://doi.org/10.1080/713803693.

Lacoste A, Cueff A, Poulet S A. 2002. P35-sensitive caspases, MAP kinases and Rho modulate β-adrenergic induction of apoptosis in mollusc immune cells. *Journal of Cell Science*, **115**(4): 761-768, https://doi.org/10.1242/jcs.115.4.761.

Launay S, Hermine O, Fontenay M et al. 2005. Vital functions for lethal caspases. *Oncogene*, **24**(33): 5137-5148, https://doi.org/10.1038/sj.onc.1208524.

Lavrik I, Golks A, Krammer P H. 2005. Death receptor signaling. *Journal of Cell Science*, **118**(2): 265-267, https://doi.org/10.1242/jcs.01610.

Letunic I, Khedkar S, Bork P. 2021. SMART: recent updates, new developments and status in 2020. *Nucleic Acids Research*, **49**(D1): D458-D460, https://doi.org/10.1093/nar/gkaa937.

Li C Y, Qu T, Huang B Y et al. 2015. Cloning and characterization of a novel *caspase*-8-like gene in *Crassostrea gigas*. *Fish & Shellfish Immunology*, **46**(2): 486-492, https://doi.org/10.1016/j.fsi.2015.06.035.

Li H L, Zhu H, Xu C J et al. 1998. Cleavage of BID by caspase 8 mediates the mitochondrial damage in the fas pathway of apoptosis. *Cell*, **94**(4): 491-501, https://doi.org/10.1016/s0092-8674(00)81590-1.

Li Z X, Wang C, Jiang F J et al. 2016. Characterization and expression of a novel caspase gene: evidence of the expansion of caspases in *Crassostrea gigas*. *Comparative Biochemistry and Physiology Part B*: *Biochemistry and Molecular Biology*, **201**: 37-45, https://doi.org/10.1016/j.cbpb.2016.07.001.

Liu F Y, Li Y L, Yu H W et al. 2021. MolluscDB: an integrated functional and evolutionary genomics database for the hyper-diverse animal phylum Mollusca. *Nucleic Acids Research*, **49**(D1): D988-D997, https://doi.org/10.1093/nar/gkaa918.

Liu W Z, Xie Y B, Ma J Y et al. 2015. IBS: an illustrator for the presentation and visualization of biological sequences. *Bioinformatics*, **31**(20): 3359-3361, https://doi.org/10.1093/bioinformatics/btv362.

Lu G X, Yu Z C, Lu M M et al. 2017. The self-activation and LPS binding activity of executioner caspase-1 in oyster *Crassostrea gigas*. *Developmental & Comparative Immunology*, **77**: 330-339, https://doi.org/10.1016/j. dci. 2017.09.002.

Matsuda I, Matsuo K, Matsushita Y et al. 2014. The C-terminal domain of the long form of cellular FLICE-inhibitory protein (c-FLIP$_L$) inhibits the interaction of the caspase 8 prodomain with the receptor-interacting protein 1 (RIP1) death domain and regulates caspase 8-dependent nuclear factor κB (NF-κB) activation. *Journal of Biological Chemistry*, **289**(7): 3876-3887, https://doi.org/10.1074/jbc.M113.506485.

Micheau O, Tschopp J. 2003. Induction of TNF receptor I-mediated apoptosis via two sequential signaling complexes. *Cell*, **114**(2): 181-190, https://doi.org/10.1016/s0092-8674(03)00521-x.

Philip N H, DeLaney A, Peterson L W et al. 2016. Activity of uncleaved caspase-8 controls anti-bacterial immune defense and TLR-induced cytokine production independent of cell death. *PLoS Pathogens*, **12**(10): e1005910, https://doi.org/10.1371/journal.ppat.1005910.

Puente X S, Sánchez L M, Overall C M et al. 2003. Human and mouse proteases: a comparative genomic approach. *Nature Reviews Genetics*, **4**(7): 544-558, https://doi.org/10.1038/nrg1111.

Qin Y P, Zhang Y H, Li X Y et al. 2020. Characterization and functional analysis of a caspase 3 gene: evidence that *ChCas* 3 participates in the regulation of apoptosis in *Crassostrea hongkongensis*. *Fish & Shellfish Immunology*, **98**: 122-129, https://doi.org/10.1016/j.fsi.2020.01.007.

Qu T, Huang B Y, Zhang L L et al. 2014. Identification and functional characterization of two executioner caspases in *Crassostrea gigas*. *PLoS One*, **9**(2): e89040, https://doi.org/10.1371/journal.pone.0089040.

Rajput A, Kovalenko A, Bogdanov K et al. 2011. RIG-I RNA helicase activation of IRF3 transcription factor is negatively regulated by caspase-8-mediated cleavage of the RIP1 protein. *Immunity*, **34**(3): 340-351, https://doi.org/10.1016/j.immuni.2010.12.018.

Ren J, Wen L P, Gao X J et al. 2009. DOG 1.0: illustrator of protein domain structures. *Cell Research*, **19**(2): 271-273, https://doi.org/10.1038/cr.2009.6.

Romero A, Novoa B, Figueras A. 2015. The complexity of apoptotic cell death in mollusks: an update. *Fish & Shellfish Immunology*, **46**(1): 79-87, https://doi.org/10.1016/j.fsi.2015.03.038.

Ronquist F, Teslenko M, van der Mark P et al. 2012. MrBayes 3.2: efficient Bayesian phylogenetic inference and model choice across a large model space. *Systematic Biology*, **61**(3): 539-542, https://doi.org/10.1093/sysbio/sys029.

Roth S, Ruland J. 2011. Caspase-8: clipping off RIG-I signaling. *Immunity*, **34**(3): 283-285, https://doi.org/10.1016/j.immuni.2011.03.011.

Salvesen G S, Dixit V M. 1997. Caspases: intracellular signaling by proteolysis. *Cell*, **91**(4): 443-446, https://doi.org/10.1016/s0092-8674(00)80430-4.

Schütze S, Tchikov V, Schneider-Brachert W. 2008. Regulation of TNFR1 and CD95 signalling by receptor compartmentalization. *Nature Reviews Molecular Cell Biology*, **9**(8): 655-662, https://doi.org/10.1038/nrm2430.

Subramanian B, Gao S H, Lercher M J et al. 2019. Evolview v3: a webserver for visualization, annotation, and management of phylogenetic trees. *Nucleic Acids Research*, **47**(W1): W270-W275, https://doi.org/10.1093/nar/gkz357.

Takeuchi O, Akira S. 2010. Pattern recognition receptors and inflammation. *Cell*, **140**(6): 805-820, https://doi.org/10.1016/j.cell.2010.01.022.

Vogeler S, Carboni S, Li X X et al. 2021. Phylogenetic analysis of the caspase family in bivalves: implications for programmed cell death, immune response and development. *BMC Genomics*, **22**(1): 80, https://doi.org/10.1186/s12864-021-07380-0.

Wajant H. 2002. The Fas signaling pathway: more than a paradigm. *Science*, **296**(5573): 1635-1636, https://doi.org/10.1126/science.1071553.

Wang J, Chun H J, Wong W et al. 2001. Caspase-10 is an

initiator caspase in death receptor signaling. *Proceedings of the National Academy of Sciences of the United States of America*, **98**(24): 13884-13888, https://doi.org/10.1073/pnas.241358198.

Wang K, Yin X M, Chao D T et al. 1996. BID: a novel BH3 domain-only death agonist. *Genes & Development*, **10**(22): 2859-2869, https://doi.org/10.1101/gad.10.22.2859.

Xiang Z M, Qu F F, Qi L et al. 2013. Cloning, characterization and expression analysis of a caspase-8 like gene from the Hong Kong oyster, *Crassostrea hongkongensis*. *Fish & Shellfish Immunology*, **35**(6): 1797-1803, https://doi.org/10.1016/j.fsi.2013.08.026.

Yang B Y, Li L L, Pu F et al. 2015. Molecular cloning of two molluscan caspases and gene functional analysis during *Crassostrea angulata* (Fujian oyster) larval metamorphosis. *Molecular Biology Reports*, **42**(5): 963-975, https://doi.org/10.1007/s11033-014-3833-y.

Yoneyama M, Fujita T. 2009. RNA recognition and signal transduction by RIG-I-like receptors. *Immunological Reviews*, **227**(1): 54-65, https://doi.org/10.1111/j.1600-065X.2008.00727.x.

Zhang G F, Fang X D, Guo X M et al. 2012. The oyster genome reveals stress adaptation and complexity of shell formation. *Nature*, **490**(7418): 49-54, https://doi.org/10.1038/nature11413.

Zhang L L, Li L, Zhang G F. 2011. Gene discovery, comparative analysis and expression profile reveal the complexity of the *Crassostrea gigas* apoptosis system. *Developmental & Comparative Immunology*, **35**(5): 603-610, https://doi.org/10.1016/j.dci.2011.01.005.

Electronic supplementary material

Supplementary material (Supplementary Tables S1–S2 and Fig.S1) is available in the online version of this article at https://doi.org/10.1007/s00343-022-2129-7.